Coupled–Channels Analyses For Heavy–Ion Fusion Reactions of ^{16}O+^{92}Zr,^{144,148}Sm Systems

M. Zamrun^{1*}, and K. Hagino^{2}

^{1}*Department of Physics, Haluoleo University, Indonesia*
^{2}*Department of Physics, Tohoku University, Sendai, Japan*

ARTICLE INFO

ABSTRACT

We study in detail the fusion reaction of ^{16}O with ^{92}Zr and ^{144,148}Sm at sub-barrier energies with coupled-channels framework using the error function potential for the nuclear potential. In particular, we investigate the effects of multiphonon excitations in target nuclei on experimental fusion cross section and barrier distributions for these reactions. We show that the present coupled-channels calculations well account for the experimental data of the fusion cross section as well as the fusion barrier distributions. It is shown that the coupled-channels calculations taking into account the coupling up to double quadrupole phonon excitations in ^{92}Zr well reproduce the experimental fusion cross section as well as fusion barrier distribution for ^{16}O+^{92}Zr. However, for ^{16}O+^{144}Sm, coupling to single quadrupole and octupole phonon states in ^{144}Sm can well explain the experimental data. And the coupling up to triple quadrupole phonon states and double octupole phonon excitations in ^{148}Sm are needed in order to reproduce the experimental data. Our study indicates the error function potential is adequate for analyses of the heavy-ion fusion reactions.

INTRODUCTION

It is now well established that the experimental cross section of heavy-ion fusion reactions between two medium heavy nuclei at energies below the Coulomb barrier are several of magnitude larger than the prediction of a potential model calculation [1]. This enhancement can be attributed to the coupling of translational motion with additional degrees of freedom such as nuclear surface vibration, rotation, and nucleon transfer and/or neck formation [2, 3] between two colliding nuclei. A standard approach to address these effects is to numerically solve the coupled channels equations by including dominant nuclear intrinsic excitations as well as transfer reactions.

Coupled-channels calculations as well as experimental data shows that the effect of nuclear intrinsic degrees of freedom can be analyzed in more detail through the so-called fusion barrier distributions [3, 1] which is defined as the second derivative of the product between the center of mass energy, E and the fusion cross section, $\sigma_{fus}(E)$, with respect to E, that is $D^{fus}(E) = d^2[E\sigma_{fus}(E)]/dE^2$. In most analyses,

both simplified [4, 5] and realistic [6, 7], coupled-channels codes have been used. In the codes, phenomenological Woods-Saxon potential has been assumed for the nuclear part of the potential. The depth, range and the surface diffuseness parameters of the potential have been determined by fitting the experimental fusion excitation functions at high energies. The double-folding model [8, 9] and the energy density functional [10, 11] has also been used for such analyses. Instead of such approaches, here we perform the coupled-channels calculations using an error function type potential for the nuclear potential. The aim of this study is to see weather this approach works to explain the fusion data of ^{16}O+^{92}Zr,^{144,148}Sm reactions [12, 13]. In particular, we study the effects of multiphonon excitations of the target nuclei on the fusion cross sections as well as the fusion barrier distributions for these systems.

COUPLED-CHANNELS FORMALISM FOR HEAVY-ION FUSION REACTIONS

In this section, we briefly describe the coupled-channels formalism for heavy-ion fusion reactions which includes the effects of the vibrational excitations of the target nucleus. The total Hamiltonian of the system is assumed to be

$^{\tau}$ Corresponding author.
  E-mail address: mzamrun@yahoo.com (M. Zamrun)

$$H = -\frac{\hbar^2}{2\mu}\nabla^2 + V_N^0(r) + \frac{Z_T Z_P e^2}{r} + H_{exct} + V_{coup}(r$$

(1)

where r is the coordinate of the relative motion between the target and the projectile nuclei, μ is the reduced mass, and ξ_T represents the coordinate of the vibration in the target nucleus. Z_P and Z_T are the atomic projectile and the target, respectively. V_N^0 is the bare of the nuclear potential. In this paper, we assumed that it is represented by an error function potential

$$V_N^0(r) = -\frac{V_0}{2}\mathrm{erfc}[(r - R_0)/a]$$

(2)

where $R_0 = r_0(A_T^{1/3} + A_P^{1/3})$ with A_P and A_T are the mass number of the projectile and target nuclei, respectively. The complementary error function is defined as

$$\mathrm{erfc}(x) = 1 - \frac{2}{\sqrt{\pi}}\int_0^x dt\, e^{-t^2}$$

(3)

In Eq.(1), H_{exct} describes the excitation spectra of the target nucleus, whereas $V_{coup}(r,\xi_T)$ is the potential for the coupling between the relative motion and the vibrational motion of the target nucleus.

In the isocentrifugal approximation [2, 5, 6], where the angular momentum of the relative motion in each channel is replaced with the total angular momentum J (in the literature, this approximation is also referred to as the rotating frame approximation or the no-Coriolis approximation), the coupled-channels equations derived from the Hamiltonian (1) read

$$\left[-\frac{\hbar^2}{2\mu}\frac{d^2}{dr^2} + \frac{J(J+1)\hbar^2}{2\mu r^2} + V_N^0(r) + \frac{Z_T Z_P e^2}{r} - E_{c.n} \right.$$

(4)

where $\in_n$ is the eigenvalue of the operator H_{exct} for the nth-channel. $V_{nm}(r)$ is the matrix elements for the coupling potential V_{coup}.

In the calculations presented below, we use the method of the computer code CCFULL [6] with the potential given by Eq.(2) and replace the vibrational coordinates ξ_T in the coupling potential, V_{coup}, with the dynamical excitation operator $\hat{O}_T$. The coupling potential is then represented as

$$V_{coup}(r,\xi_T) = V_C(r,\hat{O}_T) + V_N(r,\hat{O}_T)$$

(5)

$$V_C(r,\hat{O}_T) = \frac{3R_T^\lambda \hat{O}_T}{(2\lambda+1)r^\lambda}\frac{Z_P Z_T e^2}{r}$$

(6)

$$V_N(r,\hat{O}_T) = -\frac{V_0}{2}\mathrm{erfc}[(r - R_0 - R_T\hat{O}_T)/a] - V_N^0(r)$$

(7)

Here, $R_T = r_0 A_T^{1/3}$ is radius of target nucleus and λ denotes the multipolarity of the vibrations in the target nucleus. We have subtracted $V_N^0(r)$ in Eq. (7) to avoid the double counting.

If we truncate the phonon space up to the triple-phonon states (that is, $n = 0, 1, 2,$ and 3), the matrix elements of the excitation operator $\hat{O}_T$ in Eqs. (6) and (7) are given by

$$\hat{O}_{nm} = \begin{pmatrix} 0 & \beta_\lambda & 0 & 0 \\ \beta_\lambda & 0 & \sqrt{2}\beta_\lambda & 0 \\ 0 & \sqrt{2}\beta_\lambda & 0 & \sqrt{3}\beta_\lambda \\ 0 & 0 & \sqrt{3}\beta_\lambda & 0 \end{pmatrix}$$

(8)

where β_λ is the deformation parameter associated with multipolarity λ that can be estimated from a measured electric transition probability, $B(E\lambda)\uparrow$, from the single-phonon state ($n = 1$) to the ground state ($n = 0$). It is given by [14, 15]

$$\beta_\lambda = \frac{4\pi}{ZR_T^\lambda}\sqrt{\frac{B(E\lambda)\uparrow}{e^2}}.$$

(9)

We then assumed the harmonic oscillator model for the vibrations, where $\in_n$ in Eq.(4) is simply given by $\in_n = n\hbar\omega$.

The coupled-channels equations, Eq.(4), are solved with incoming wave boundary condition for $u_n(r)$

$$u_n(r) \sim T_n \exp\left[-i\int_{r_{abs}}^r k_n(r')dr' \right]; \quad r \le r_{abs}$$
$$\rightarrow H_J^{(-)}(k_n r)\delta_{n0} + R_n H_J^{(+)}(k_n r); \quad r \rightarrow \infty$$

(10)

where T_n and R_n are the transmission and reflection coefficients, respectively. $H_J^{(-)}$ and $H_J^{(+)}$ are the incoming and outgoing Coulomb wave functions, respectively. The local wave number for n-th channel is given by

$$k_n(r) = \sqrt{\frac{2\mu}{\hbar^2}\left[E_{c.m.} - \in_n - \frac{J(J+1)\hbar^2}{2\mu r^2} - V_N^0(r) - Z\right]}$$

,(11)

and $k_n = k_n(r = \infty)$. When the transmission coefficients is found then the transmission probability can be calculated as

$$P_J(E_{c.m.}) = \sum_n \frac{k_n(r_{abs})}{k_0}|T_n|^2 \qquad (12)$$

where $k_0 = \sqrt{2\mu E_{c.m.}/\hbar^2}$. Finally, the fusion cross section is calculate as

$$\sigma_{fus}(E_{c.m.}) = \frac{\pi}{k_0^2}\sum_J(2J+1)P_J(E_{c.m.}) . \qquad (13)$$

The fusion barrier distribution is calculated using point different formula [12] with $\Delta E_{c.m.} = 2 \text{ MeV}$.

We will apply this formalism in the next section to analyze the heavy-ion fusion data of ^{16}O+^{92}Zr,^{144,148}Sm systems.

RESULTS AND DISCUSSION

In this section we present our detailed coupled-channels analyses for heavy-ion fusion data of ^{16}O+^{92}Zr,^{144,148}Sm systems [12, 13]. The calculations are done with the computer code CCFULL [6] but using the potential given by Eq. (2). As usually done, the parameters of the nuclear potential are determined by fitting the experimental fusion cross section data at high energies for each reaction in one dimensional calculation. The

optimum value for V_0 , r_0 , and a parameters and the corresponding Coulomb barrier, V_B , are summarized in Table 1. In the calculations we only include the excitation of the target nuclei while the excitation of ^{16}O is not explicitly taking into account. This is a general features for fusion reactions that using the ^{16}O as a projectile where its effects can be incorporated in fitting the parameters of nuclear potential [16].

$^{16}O+^{92}Zr$ System

Let us now discuss the reaction of ^{16}O+^{92}Zr. In performing the coupled-channels calculations, we include only the quadrupole (2^+) phonon excitation of ^{92}Zr. The eigenvalue for the H_{exct} in Eq.(4) is taken to be $\in_n = n_2 \in_2$ where n_2 is the number of quadrupole phonon and $\in_2$ its excitation energy, i.e. $\in_2 = 0.934$. The corresponding deformation parameter calculated using Eq.(9) with $r_0 = 1.06$ is found to be $\beta_2^C = 0.132$. Following Ref. [17] which found that $\beta_2^N > \beta_2^C$ is needed for explaining the inelastic scattering data of ^{16}O+^{92}Zr reaction, we then varied the value of β_2^N from $\beta_2^N = \beta_2^C$ in order to optimize the fit to the experimental fusion data for the system.

The results of coupled-channels calculations are compared with the experimental data in Fig. 1. Fig. 1(a) and 1(b) show the fusion cross sections and the fusion barrier distributions, respectively. The dot-dashed line is the results of

Table 1. The optimum parameters for the nuclear potential for ^{16}O+^{92}Zr,^{144,148}Sm systems obtained by fitting the fusion cross section data with fixed a = 2.7 fm. The resultant Coulomb barrier V_B is also listed.

System	$V_0 (\text{MeV})$	$r_0 (\text{fm})$	$a (\text{fm})$	$V_B (\text{MeV})$
^{16}O+^{92}Zr	285	0.83	2.7	42.00
^{16}O+^{144}Sm	215	0.90	2.7	61.25
^{16}O+^{148}Sm	227	0.91	2.7	60.25
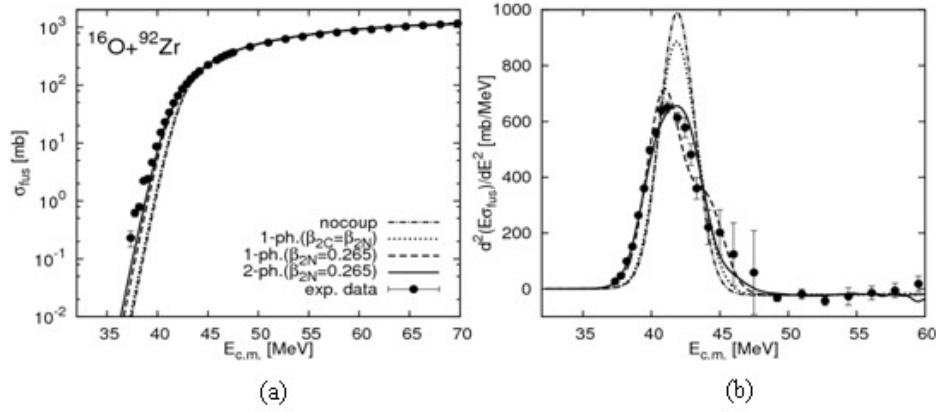
Fig. 1. Comparison of the experimental data and the coupled-channels calculations for ^{16}O+^{92}Zr reaction for (a) the fusion cross section and (b) the fusion barrier distribution. The dot-dashed line is the results of one dimensional calculation while the dotted line is obtained by including the coupling of single quadrupole phonon state with $\beta_2^N = \beta_2^C = 0.132$. The dashed and solid lines are obtained by including coupling up to single and double quardupole excitations in ^{92}Zr with $\beta_2^N = 0.265$, respectively. Experimental data are taken from Newton et al.[13].

one dimensional model. The results of coupled-channels calculations taking into account the coupling to single quadrupole phonon excitation in ^{92}Zr with $\beta_2^N = \beta_2^C = 0.132$ is denoted by the dotted line. As we see, it fails to reproduce the experimental data of the fusion cross section as well as the fusion barrier distribution. We have checked that the situation is still similar even the coupling up to double quadrupole phonon states is taking into account. We then repeat the calculations including coupling to the single phonon state but we varied the value of β_2^N in order to achieve the best fit with the data. The result is given by the dashed line. Now the agreement between the calculations and the experimental data are improved in this way and we found the optimum value for β_2^N, that is $\beta_2^N = 0.265$. However, the theoretical barrier distribution is still somewhat differs with the data. It has a slight structure at energy around 45 MeV which is absent in the experimental data. We then investigate the effects of double quadrupole phonon excitations in the target nucleus and using $\beta_2^N = 0.265$. The calculated fusion cross section and the fusion barrier distribution is given by the solid line in Fig. 1. Now the calculations are well reproduced the experimental data for the fusion cross section as well as the fusion barrier distributions. It is thus evident that the coupling to the double quadrupole phonon states in target nucleus with $\beta_2^N > \beta_2^C$ is needed to explain the experimental fusion data of ^{16}O+^{92}Zr reaction. This is somewhat differs with the one found in Newton et al.[13] where the coupling to single octupole phonon excitation in addition to double

quadrupole phonon states in ^{92}Zr is necessary for reproducing the experimental data. The difference between Newton's results.[13] and the present calculations may originate from the fact that they used a larger radius $R_T (=1.2 A_T^{1/3} \text{ fm})$ and thus a small value for $\beta_2^C = 0.103$. Also the anharmonicity of nuclear vibrations may play a role in this reaction which has been found in other systems [18 - 21]. It is beyond the scope of this paper and we will leave it for a future study.

^{16}O+^{144}Sm System

We now discuss the heavy-ion fusion reaction of ^{16}O+^{144}Sm system. In the coupled-channels calculations of fusion cross section as well as fusion barrier distribution, we include the lowest states of the ^{144}Sm, that is the 2^+ (quadrupole) and 3^- (octupole) states. The eigenvalue for H_{exct} in Eq. (4) is simply taken to be $\epsilon_n = n_2 \epsilon_2 + n_3 \epsilon_3$ where n_2 and n_3 are the number of quadrupole and octupole phonons, respectively. ϵ_2 and ϵ_3 are the excitation energy of the quadrupole and the octupole phonon excitations, i.e., $\epsilon_2 = 1.66$ MeV and $\epsilon_3 = 1.81$ MeV, respectively. The deformations parameters are estimated to be $\beta_2 = 0.11$ and $\beta_3 = 0.21$ using Eq.(9) with radius parameter $r_0 = 1.06$. In the calculation presented below and in the next subsection, we take $\beta^N = \beta^C$ for the quadrupole and octupole deformations.
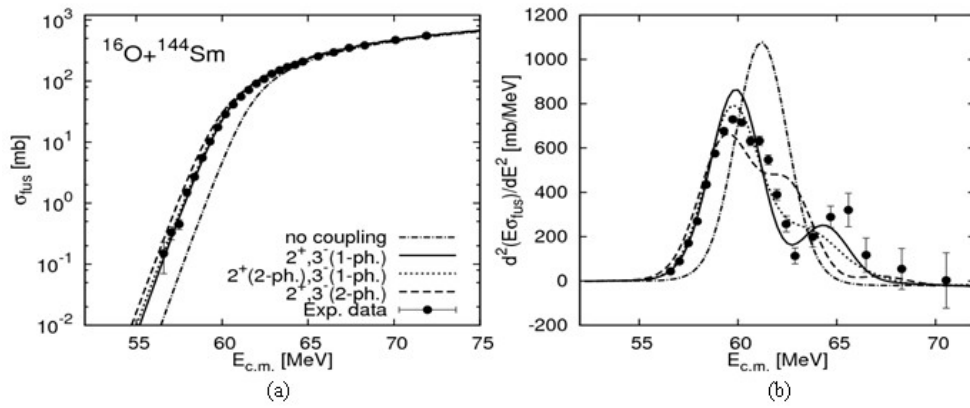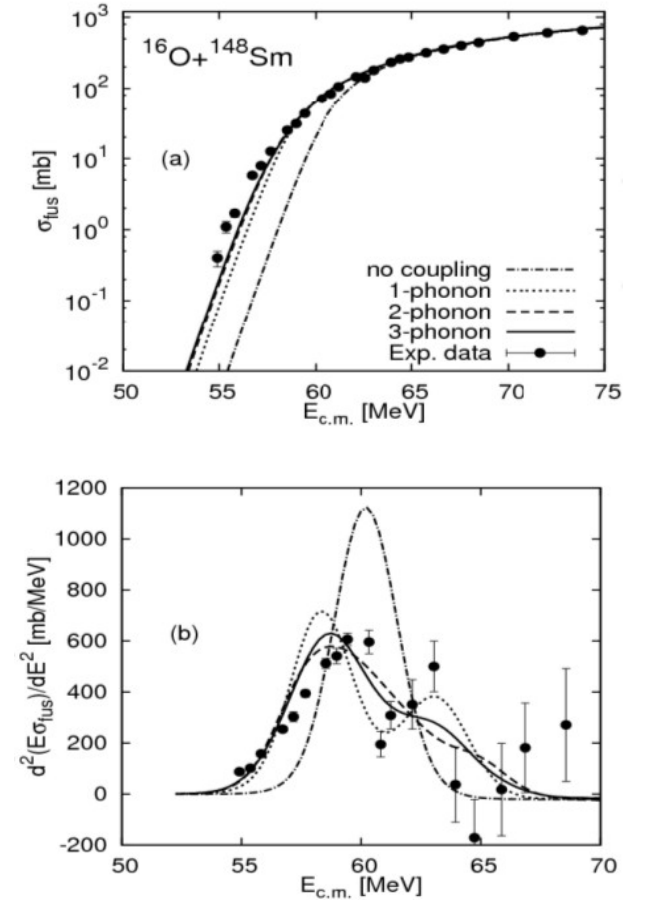
Fig. 2. Comparison of coupled-channels calculations with experimental data for $^{16}O+^{144}Sm$ for (a) the fusion cross section and (b) the fusion barrier distribution. The dot-dashed line is the result of one dimensional calculation. The coupled-channels calculations which take into account the coupling to single quadrupole and octupole excitations in ^{144}Sm is given by solid line. The dotted line is obtained by including the coupling to double quadrupole phonon excitations in addition to single octupole state in target nucleus. And the dashed line is the results when coupling to quadrupole and octupole phonon excitation is truncated up to double phonon states. Experimental data are taken from Leigh et al.[12].

The results of coupled-channels calculations are compared with the experimental data in Fig. 2. Fig. 2(a) and 2(b) shows the fusion cross section and the fusion barrier distribution, respectively. The solid line represents the results of the calculations taking the single phonon state of the quadrupole and octupole excitations into account. The mutual excitation, $2^+ \otimes 3^-$, is neglected. The calculations including the double quadrupole phonon states in addition to single octupole vibration is shown by dotted line. We also take the mutual excitation, $2^+ \otimes 3^-$ state, into account. And the dashed line is obtained when coupling to double quadrupole and octupole phonon states and the mutual excitation, $2^+ \otimes 3^-$ state, is included in the coupled-channels calculations. Fig. 2(a) shows that all the three calculations well reproduce the experimental fusion cross section. However, the clear difference can be seen if we compare the obtained fusion barrier distributions (see Fig. 2(b)). The first calculations (the solid line in Fig. 2(b)) agree well with experimental data where the high energy peak at energy around $E = 65$ MeV is reproduced. However, the other two calculations (the dotted and the dashed lines in Fig. 2(b)) fail to explain the experimental data. This clearly demonstrates the possible danger of analyzing the experimental fusion data in a form of fusion cross section alone. It is well known that the fusion barrier distribution is very sensitive to the detailed channel coupling [12]. It thus evident that the coupling to single quadrupole and octupole excitations in ^{144}Sm is necessary for explaining the experimental fusion data of ^{16}O+^{144}Sm reaction as long as we assume the harmonic limit for the nuclear vibrations. It has been shown in Refs.[19, 20, 2] that the anharmonicities of double phonon excitations in ^{144}S play an important role when the Woods-Saxon potential is used as a nuclear part of the interaction in the coupled-channels calculations. It is an interesting task to study such effect with the present coupled-channels approach. The work toward this problem is in progress and we will publish it on a separate paper.

^{16}O+^{148}Sm System

In this subsection, we present our detailed coupled-channels analyses for ^{16}O+^{148}Sm fusion reaction. We especially investigate the role of multiphonon excitations in the target nucleus, ^{148}Sm, on fusion cross section as well as fusion barrier distribution. In performing the calculations, we include the 2^+ (quadrupole) and 3^-

(octupole) states of ^{148}Sm whose excitation energy $\in_2 = 0.55$ MeV and $\in_3 = 1.16$ MeV, respectively. Again the corresponding deformations parameters are estimated using Eq.(9) with radius parameter $r_0 = 1.06$ and they are found to be $\beta_2 = 0.182$ and $\beta_3 = 0.236$, respectively. And we take the eigenvalue for H_{exct} in Eq.(4) to be

$$\in_n = n_2 \in_2 + n_3 \in_3$$

where n_2 and n_3 are the number of quadrupole and octupole phonons, resepectively.


Fig. 3. Effects of multi-quadrupole phonon excitations on fusion cross section (a) and fusion barrier distribution (b) for ^{16}O+^{148}Sm system. The dotted and dashed lines are results of coupled-channels calculations taking into account single and double quadrupole phonon excitations in ^{148}Sm, respectively. The solid line is obtained by including the coupling up to triple quadrupole phonon states. In all calculations, coupling to octupole phonon excitation is truncated up to single phonon state. It is also shown the result of one dimensional calculation (dot-dashed line). Experimental data are taken from Leigh et al.[12].

The dotted line in Fig. 3 shows the results of coupled-channels calculations obtained by taking into account the coupling to the single quadrupole and octupole excitations in the target nucleus.

The mutual excitation, $2^+ \otimes 3^-$ state, is ignored in respectively. It is apparent that the calculations are inconsistent with data. The obtained fusion cross sections underestimate the experimental data at low nergies and the obtained fusion barrier distribution fails to reproduce the data. We then repeat the calculations by including the coupling up to double phonon states of the quadrupole excitations in addition to coupling to single octupole phonon state. We take into account the $2^+, 3^-, 2^+ \otimes 3^-$ and $2^+ \otimes 2^+$ states in the calculations. The result is denoted by the dashed line in Fig. 3. When the coupling up to triple quadrupole phonon states is taking into account then we get the solid line in Fig. 3. We include $2^+, 3^-, 2^+ \otimes 3^-, 2^+ \otimes 2^+ \otimes 3^-$ and $2^+ \otimes 2^+ \otimes 2^+$ states in the calculations. From these two calculations, it is seen that the agreement with the experimental fusion cross section is improved whereas the obtained fusion barrier distributions still inconsistent with the data. However, it is difficult to distinguish the effect between the double and triple quadrupole phonon excitations since the obtained fusion cross sections as well as the fusion barrier distributions are similar to each other.
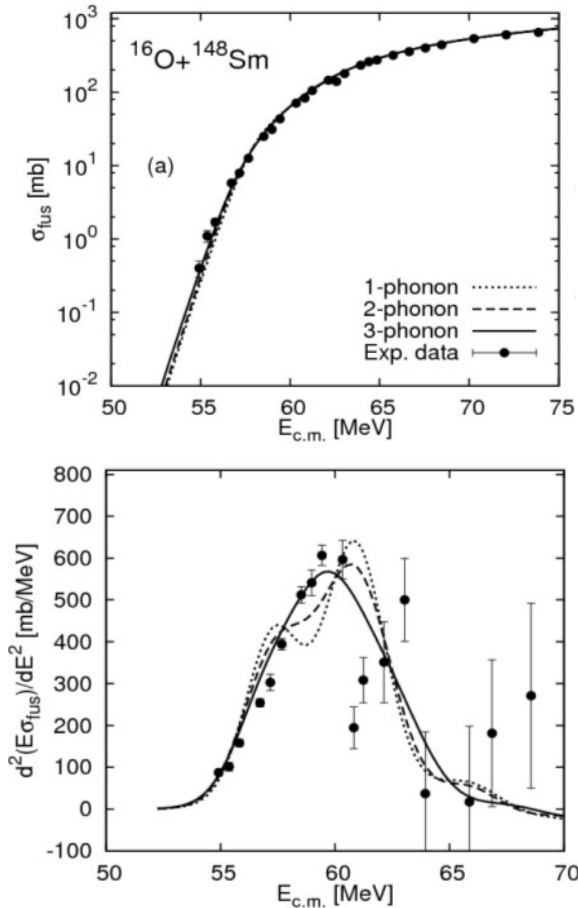
this way. Fig. 3(a) and 3(b) show the fusion cross section and the fusion barrier distribution,

Fig. 4. The same as Fig. 3 but coupling to the octupole phonon excitations is included up to double phonon states. Experimental data are taken from Leigh et al.[12].

As previously found that the results of coupled-channels calculations taking into account the coupling to double and triple quadrupole phonon states while keeping the coupling to single octupole phonon state of the target nucleus are resemble to each other, we then investigate the effects of the double octupole phonon excitations of the target nucleus. Fig. 4 show the role of the double octupole phonon states with various coupling schemes for quadrupole phonon state. Fig. 4(a) and 4(b) shows the fusion cross sections and the fusion barrier distributions, respectively. The dotted line is obtained when coupling to single quadrupole phonon and double octupole phonon states and the mutual excitation, $2^+ \otimes 3^-$ state, are taking into account. The dashed and solid lines are obtained by taking into account the coupling to double and triple quadrupole phonon states in addition to the coupling of double octupole phonons, respectively. In the first case, we include 2^+, 3^-, $2^+ \otimes 3^-$, $2^+ \otimes 2^+$, $2^+ \otimes 2^+ \otimes 3^-$, and $3^- \otimes 3^-$ states while in later case the 2^+, 3^-, $2^+ \otimes 3^-$, $2^+ \otimes 2^+$, $2^+ \otimes 2^+ \otimes 3^-$, $2^+ \otimes 2^+ \otimes 2^+$, $2^+ \otimes 2^+ \otimes 2^+ \otimes 3^-$, $3^- \otimes 3^-$, and $2^+ \otimes 3^- \otimes 3^-$ states are taking into account. It is clear that the calculations with coupling to single, double, and triple quadrupole phonon states in addition to the coupling to octupole phonon states well reproduce the experimental fusion cross sections (see Fig. 4(a)). They almost fit the data with the same quality. The different between them can be seen more clearly if we compare the obtained fusion barrier distributions (see Fig. 4(b)). It is apparent that the coupled-channels calculations with the triple quadrupole and double octupole phonon states well agree with the experimental fusion barrier distribution (the solid line in Fig. 4(b)). It is thus evident that the triple quadrupole and double octupole phonon excitations in [148]Sm is important for explaining the experimental fusion data of [16]O+[148]Sm reaction. Min Liu et al.[10] has shown that the anharmonicities of the phonon vibrations in [148]Sm plays an important role in describing the experimental data for this system when performing the coupled-channels calculations using the phenomenological Woods-Saxon potential. It is thus an interesting future subject to study those effects with the present coupled-channels formalism.

CONCLUSIONS

We have performed a detailed coupled-channels analysis for heavy-ion fusion reactions of the ^{16}O+^{92}Zr,^{144,148}Sm systems using the error function potential for the nuclear potential. Our coupled-channels calculations with multiphonon excitations of the target nucleus and assumed the harmonic spectra for the nuclear vibrations well reproduce the experimental fusion cross sections as well as fusion barrier distributions for the systems studied in this paper. This is clearly indicates that the error function potential is adequate for coupled-channels analysis of heavy-ion fusion reactions.

In more details, the calculations with coupling up to double phonon states with $\beta_2^N > \beta_2^C$ in ^{92}Zr well reproduce the experimental data for ^{16}O+ ^{92}Zr system. However, for ^{16}O+^{144,148}Sm systems, the value of β^N is equal to β^C both for quadrupole (β_2) and octupole (β_3) deformations. We found that the calculations taking into account the coupling to single quadrupole and octupole phonon excitations in ^{144}Sm is important to fit the experimental data of ^{16}O+^{144}Sm system. And for the ^{16}O+^{148}Sm system, the coupled-channels calculations with the coupling to triple quadrupole phonon excitations in addition to double octupole phonon states in ^{148}Sm seems to be needed for describing the experimental data.

Although our present coupled-channels calculations well account for the experimental data for the systems studied in this paper, care has to be taken concerning the anharmonicity of the vibration in the target nucleus. A further detailed investigations will necessarily take into account the anharmonicity of multiphonon excitations which have been reported to play a crucial role in heavy-ion fusion reaction [18 - 20] as well as quasi-elastic scattering at backward angle [20, 21].

ACKNOWLEDGEMENTS

REFERENCES

1.   M. Beckerman, Rep. Prog. Phys. **51** (1988) 1047.

2.   A.B. Balantekin and N. Takigawa, Rev. Mod. Phys. **70** (1998) 77.

3.   N. Rowley, G. R. Sacthler, and P. H. Stelson, Phys. Lett. B **254** (1991) 25.

4.   C.H. Dasso, and S. Landowne, Comput. Phys. Commun. **46** (1987) 187.

5.   J. Fernandes-Nielo, C.H. Dasso, and S. Landowne, Comput. Phys. Commun. **54** (1989) 409.

6.   K. Hagino, N. Rowley and A.T. Krupta, Comput. Phys. Commun. **123** (1999) 143.

7.   I.J. Thompson, Comput. Phys. Rep. **7** (1988) 167.

8.   I.I. Gontchar, D.J. Hinde, M. Dasgupta, and J.O. Newton, Phys. Rev. C **73** (2006) 1.

9.   I.I. Gontchar, D.J. Hinde, M. Dasgupta, and J.O. Newton, Phys. Rev. C **69** (2004) 1.

10.   Min Liu, Ning Wang, Zhuxia Li, Xizhen Wu, and Enguang Zhao, Nucl. Phys. A **768** (2006) 80.

11.   F.Muhammad Zamrun, K. Hagino, and N. Takigawa, *AIP Conference Proceeding* **856** (2006) 309.

12.   J.R. Leigh, M. Dasgupta, D.J. Hinde, J.C. Mein, C.R. Morton, R.C. Lemmon, J.P. Lestone, J.O. Newton, H. Timmers, J.X. Wei, and N, Rowley, Phys. Rev. C **52** (1995) 3151.

13.   J.O. Newton, C.R. Morton, M. Dasgupta, J.R. Leigh, J.C. Mein, D.J. Hinde, and H. Timmers, Phys. Rev. C **64** (064608) (2001) 1

14.   T. Kibedi, and R.H. Spears, At. Data Nucl. Data Tables **80** (2002) 35.

15.   S. Raman, C.W. Nestor, and P. Tikkanen, At. Data Nucl. Data Tables **78** (2001) 1.

16.   K. Hagino, N. Takigawa, M. Dasgupta, D.J. Hinde, And J.R. Leigh, Phys. Rev. Lett. **79** (1997) 2014.

17.   E.M. Takagui, G.R. Satchler, H. Takai, K. Koide, and O. Ietzsh, Nucl. Phys. A **514** (1990) 120.

18.   K. Hagino, S. Kuyucak, and N. Takigawa, Phys. Rev. C **57** (1998) 1349.

19.   K. Hagino, N. Takigawa, and S. Kuyucak, Phys. Rev. Lett. **79** (1997) 2943.

20.   F. Muhammad Zamrun and K. Hagino, *AIP Conference Proceeding* **1150** (2009) 464.

21.   F. Muhammad Zamrun and K. Hagino,
        Phys. Rev. C **77** (2008) 1.